

Investigations on Scalable Fabrication Procedures for Self-Sensing Carbon Nanotube Cement-Matrix Composites for SHM Applications

Antonella D'Alessandro, Marco Rallini, Filippo Ubertini¹, Annibale Luigi Materazzi,
Josè Maria Kenny

Department of Civil and Environmental Engineering, University of Perugia, Perugia, 06125, Italy

Abstract.

Electrically conductive cement-based composites doped with carbon nanotubes possess the functional properties of being strain- and damage-sensitive, thus providing a cost-effective solution for monitoring of concrete structures. The weak point of the technology is the dispersion of the nanotubes, typically based on special procedures, such as sonication, that are not suitable for large scale applications. This paper presents a systematic investigation on various procedures for fabricating carbon-nanotube-cement pastes, mortars and concretes. Dispersion of nanotubes in water is achieved using chemical dispersants and different mixing strategies, while quality of nanotubes' dispersion is assessed by measuring the rate of nanotube separation and by SEM inspections. Electrical percolation and strain-sensitivity are investigated in order to assess the quality of the fabricated composites. The results of this research allow to identify a processing procedure that, without sonication, might be potentially effective for fabricating self-sensing cement-based composites in a way that is compatible with large scale deployment. In particular, similarly to what observed in the case of sonicated specimens, the percolation thresholds of mortars and concretes fabricated with the "scalable" procedure are seen to be around 1% w. of MWCNTs

¹ Corresponding author, e-mail: filippo.ubertini@unipg.it

content with respect of the weight of cement, while the same percolation threshold is less evident for pastes. Electrical conductivity and gauge factor of the same samples are also similar to those of sonicated composites, whereby conductivity of composite pastes, mortars and concretes assumes values of $5.2\text{E-}4$, $1.8\text{E-}4$ and $1.0\text{E-}4$ (Ωcm)⁻¹, respectively, while gauge factors are equal to 130, 68 and 23, respectively.

Keywords: Smart Concrete, Composite, Crack Detection, Dispersion, Electrical Properties, SEM

1. INTRODUCTION

Structural Health Monitoring (SHM) is the automated condition assessment of structures through observation and analysis of data collected on-site by sensing systems [1]. It has an enormous economic potential because it enables condition-based maintenance instead of prevention-based or breakdown-based maintenance [2].

SHM is far from being broadly implemented, despite of the considerable research effort carried out in recent years [3, 4, 5, 6] in order to tackle the advanced state of degradation of infrastructural systems in western countries [1]. The main bottleneck of current SHM technologies is that they are hardly scalable to large scale structures because of management and maintenance issues, and because the number of sensors that are necessary for an effective health assessment rapidly increases with increasing structural size [7].

Recent advances in the field of Nanotechnology have led to the development of new multifunctional and smart materials that have tremendous potential in SHM [8-9]. Especially interesting are conductive cement-based composite materials that display self-sensing abilities, whereby their electrical response is modulated by their state of strain [10-18]. The technology of self-sensing nanocomposite cement-based materials is especially suitable for the transformation of concrete structures into self-sensing systems, by transforming the structural surfaces into infinite sets of potential embedded sensors with enhanced durability and ease of utilization. However, there

are still issues to be resolved before large-scale deployment of such a sensing technology can be achieved.

Self-sensing cement-based composites are based on the incorporation of short fibers [11-13], as well as micro- and nano-inclusions into cementitious matrices, mostly using carbon-based materials [14], to provide electrical conductivity [8-33]. Particularly promising are self-sensing cement-based materials incorporating Multi Walled Carbon NanoTubes (MWCNTs) [34,35], which enable the transduction of a mechanical strain into a measurable variation of the electrical resistance [10]. The authors have recently developed a sensor based on a multifunctional cement-based composite material, termed Carbon NanoTube Cement-based Sensor (CNTCS) [28-31], capable of dynamic strain sensing. The main bottleneck limiting large-scale applications of such a sensing technology is related to the difficulties in obtaining a good dispersion of particle additives that typically requires special treatments, such as sonication, that are hardly scalable to large casting volumes. The difficult dispersion of the nanotubes is related to the circumstance that MWCNTs tend to form agglomerates and bundles due to the electronic configuration of tube walls and their high specific surface area, which enhances Van der Waals attraction forces among nanotubes [36,37]. Although the use of dispersing additives can help preventing the formation of bundles in an aqueous solution containing Carbon NanoTubes (CNTs), most authors agree that ultrasonic treatment is compulsory to achieve a satisfactory dispersion [38,39].

The self-sensing ability of cement-based nanocomposites is strictly related to their electrical conductivity, which is achieved when the properly dispersed nanotubes reach a critical threshold, termed the percolation threshold [40,41]. The percolation threshold also roughly represents the optimal quantity of nanotubes that is necessary to achieve a good self-sensitivity, being electrical conduction dominated by the nanotubes' percolating path above percolation and the material being almost an electrical insulator below percolation [34].

This paper presents an in-depth study on electrical conductivity and strain sensing ability of cement pastes, mortars and concretes doped with MWCNTs and prepared using different

fabrication processes. The aim is to define a preparation strategy suited for fabricating conductive cement-based composites with improved scalability to large-scale applications, possibly using dispersing additives, but limiting special treating procedures such as sonication.

The rest of the paper is organized as follows. Section 2 gives a background on carbon nanotube cement-based composites, with focus on preparation issues and sensing principle. Section 3 presents materials' properties, preparation strategies and characteristics of specimens fabricated in this study. Section 4 presents an experimental methodology to assess the effect of the preparation strategy on nanotubes' dispersion and to investigate conductivity, percolation and strain-sensitivity of the composite materials. Section 5 presents experimental results and Section 6 concludes the paper.

2. CARBON NANOTUBE CEMENT-BASED COMPOSITES

Carbon nanotube cement-based composites, such as pastes, mortars and concretes, are obtained by doping traditional admixtures with carbon nanotubes. Such nanoinclusions provide the composite material with piezoresistive strain-sensing and thus damage-sensing capabilities. In what follows, issues arising in materials' preparation, mostly related to the proper dispersion of the nanotubes, and strain sensing principle are briefly reviewed, focusing on composites based on the use of MWCNTs.

2.1. Materials' preparation issues

MWCNTs can be included in the structural family of Fullerene. Due to sp^2 ibridation, the carbon atoms are arranged in a hexagonal pattern, bonded together with strong covalent bonds, type σ - σ . The last valence electrons form π bonds, producing Van der Waals forces between the tubes. Van der Waals attractive forces cause the formation of bundles [39,42-45] that highly complicate the process of achieving a uniform dispersion of the nanotubes within the cement matrix.

Insufficient dispersion of the nanotubes results in composites with defects, insufficient mechanical properties and low strain-sensitivity. On the contrary, uniform dispersion enhances the

interaction between nanotubes and matrix, due to the increase of the interfacial contact area, and creates an electrically conductive network through the nanotubes that is responsible for the piezoresistive behavior.

Dispersion of the nanotubes is accomplished in water, at first, prior to the addition of cement powder, aggregates and additives. There are three different approaches to disperse the nanotubes in water [46]: (i) mechanical methods, based on the use of mechanical mixers that separate the nanotubes; (ii) physical methods, based on the use of dispersants that operate a non-covalent surface modification; (iii) chemical methods, through a covalent surface modification. Mechanical agitation by ultrasonication produces temporary dispersion of nanotubes [47,48]. Therefore, in many cases, the sonic treatment complements chemical or physical methods. Chemical treatments (covalent) use aggressive chemicals, such as neat acids, that operate a functionalization of MWCNT surface. The MWCNTs with attached functional groups are less likely to agglomerate but could have defects or alterations due to the chemical treatment. On the contrary, physical (non-covalent) dispersants do not alter the covalent bonds on the tube lattice because the dispersing chemical groups are physically attached onto the MWCNTs' surface.

In this paper, physical methods are applied in combination with mechanical mixing, and the results are compared with those obtained when physical methods are complemented with sonic treatment.

2.2. Sensing principle

When cement-based nanocomposite materials doped with MWCNTs are subjected to a variation in their internal state of strain, the distance between the nanotubes is changed, which also changes their electrical interactions and, in particular, the tunneling effects that are responsible for electrical conductivity [50-53]. This corresponds to a variation in materials' electrical resistivity that can be measured via a data acquisition system.

Although the composite materials are not only resistive, but also capacitive due to materials' dielectric properties and to the presence of double layer phenomena around electrodes, literature findings [54] allow to hypothesize that only the internal resistance is influenced by the mechanical deformation. Henceforth, the relationship between incremental variation in electrical resistance, ΔR , and axial strain, ε (positive in compression), can be modeled in analogy with electrical strain gauges as

$$\frac{\Delta R}{R_0} = -\lambda \varepsilon \quad (1)$$

where R_0 is the unstrained internal electrical resistance and λ is the gauge factor of the material. Linearity of Eq. (1) results from the assumption of sufficiently small deformations. Literature results show, for cement-based composites doped with MWCNTs, values of the gauge factor ranging from about 12 for mortars and concretes (see for example ref. [49]), up to about 400 for pastes (see for example ref. [25]), so, in this last case, up to two orders of magnitude greater than gauge factors of typical electric strain gauges.

It is noted from Eq. (1) that the sensitivity, S , of transducers made of nanocomposite cement-based materials is given by

$$S = \frac{\Delta R}{\varepsilon} = -\lambda R_0 \quad (2)$$

The optimal content of nanotubes is the one that maximizes S in Eq. (2). If the content of nanotubes is greater than this optimal value, the nanoparticles form a continuous network and S decreases because of a drastic decrease in R_0 . On the contrary, if the content of nanotubes is smaller than the optimal value, the distance between nanotubes is too large for strain sensing and λ decreases. Literature results suggest that the optimal content of nanotubes is around the percolation threshold [50].

3. MATERIALS AND SPECIMENS' PREPARATION

Specimens made of composite cement paste, mortar and concrete doped with MWCNTs were prepared using different fabrication procedures and different contents of nanotubes. Key aspects of the preparation procedure were changed with the purpose of assessing their effects over nanotube dispersion and quality of the fabricated composites. Those aspects are: type and amount of dispersant and type of mixing procedure.

In this section the main physical and chemical characteristics of the adopted MWCNTs, the types of dispersants used in the fabrication of the specimens, the preparation procedures and the specimens characteristics are reported.

3.1. Carbon Nanotubes

Multi-walled carbon nanotubes type Graphistrength C100 from Arkema were used as conductive nanoinclusions in the cementitious matrices. MWCNTs appear as a black powder, made of agglomerated nanostructures, with a very low apparent density. They provide a larger strain sensitivity in comparison to single-walled nanotubes because of their cylindrical structure consisting of coils of atomic layers of graphite [47,55,56]. Table 1 summarizes the main physical, chemical and mechanical properties of the MWCNTs adopted in the fabrication process.

Table 1. Main characteristics of MWCNTs used in the experiments (from [56])

Geometrical Property	Value	Chemical/Physical property	Value
Mean agglomerate size	200–500 μm	Carbon content	>90% In weight
Mean number of walls	5–15	Free amorphous carbon	Undetectable (SEM)
Outer mean diameter	10–15 nm	Surface area	100-250 m^2/g
Length	0.1–10 μm	Apparent density	50–150 kg/m^3
Mechanical Property	Value	Weight loss at 105 °C	<1%
Young Modulus	> 1 TPa	Thermal Conductivity	> 3000 W/(mK)
Tensile strength	About 150 GPa	Electrical Conductivity	up to $10^7 (\Omega\text{m})^{-1}$

3.2. Dispersants

Nine different types of dispersants were considered in the experiments, as summarized in Table 2. Dispersant number 1 is a dispersing additive for particles in aqueous emulsions consisting of a solution of an ammonium salt of an acrylate copolymer. Dispersant number 2 is a second generation superplasticizer based on polycarboxylate ethers. The third dispersant is a wetting and dispersing additive for aqueous solutions or emulsions with different types of pigments. It is a solution of block copolymers with a high molecular weight and pigment affinic groups. The fourth additive is a dispersing agent composed of alkylammonium salt of a high molecular-weight copolymer particularly suitable for carbon black particles. The fifth dispersant, sodium dodecylbenzenesulfonate, is a colourless salt with surfactant properties, constituted by a series of organic compounds. Dispersant number 6 is composed by sodium lignosulfonate (lignosulfonic acid, sodium salt), while the 7th one (polystyrene sulfonates) is made of polymers derived from polystyrene with sulfonate functional groups, which is a particular dispersant for metal oxides, carbonates and sulfates, and a suspending agent for particles. The 8th dispersant, polyvinyl alcohol (PVA), is a water-soluble synthetic polymer. Finally, dispersant number 9 is a water-soluble non-ionic surfactant and detergent consisting of a hydrophilic polyethylene oxide chain and an aromatic hydrocarbon group.

Table 2. Dispersants used in the experiments

No.	Additive Name	Description
1	BYK 154	Ammonium polyacrylate-based
2	G.SKY 624	Polycarboxylate ether-based
3	DISPERBYK 190	High molecular weight block copolymer with pigment affinic groups
4	BYK 9076	Alkylammonium salt of a high molecular-weight copolymer
5	NaDDBS	Sodium dodecylbenzenesulfonate

6	SLS	Lignosulfonic acid sodium salt
7	PSS	Polystyrene sulfonates
8	PVA	Polyvinyl alcohol
9	NaDDBS-TX100	Combination of sodium dodecylbenzenesulfonate and copolymers of polyethylene oxide and aromatic hydrocarbon group

3.3. Preparation procedures

As the first step of all considered preparation procedures, 0.1 g of MWCNTs and a variable amount of chemical dispersant were added to 40 g of deionized water. The chosen amount of MWCNTs corresponds to about the 0.1% with respect to the mass of cement, assuming a water/cement ratio of 0.4. Three different concentrations for each dispersant were considered, namely 0.1:1, 1:1 and 10:1 compared to the mass of MWCNTs, corresponding to 0.01 g, 0.1 g and 1.0 g of dispersant. Premixing of deionized water, dispersant and MWCNTs was manually accomplished and followed by 10 minutes of magnetic stirring. Two different procedures were then considered for mixing MWCNTs in water and they are named as follows:

- mixing procedure ME,
- mixing procedure SO.

Mixing procedure ME was a mechanical mixing, while mixing procedure SO consisted of a sonication procedure. In mixing procedure ME, after magnetic stirring, the water-dispersant-MWCNTs suspension was mechanically mixed for 60 minutes, while, in mixing procedure SO, after magnetic stirring, the water-dispersant-MWCNTs suspension was sonicated for 30 minutes.

Figure 1 reports a sketch of the considered preparation procedures.

Considering the nine different types of dispersants, the three different amounts of dispersants and the two mixing procedures, a total of $9 \times 3 \times 2 = 54$ different combinations were obtained. For each of them, the quality of the dispersion of the nanotubes was investigated through the methodology presented in the following section.

The different samples of MWCNTs-water dispersions prepared for the experiments were named using the following identification code: "MP_DN_DR", where MP denotes the mixing procedure, that can be either ME or SO, as described above, DN is the dispersant number (see Table 2) and DR, for dispersants from 1 to 8, is the ratio between dispersant and MWCNTs mass (that can be 0.1:1, 1:1 and 10:1), while, for dispersant 9, it is expressed as 10:1(X), where 10:1 is the fixed ratio between NaDDBS and MWCNTs mass and X is the ratio between TX100 and MWCNTs.

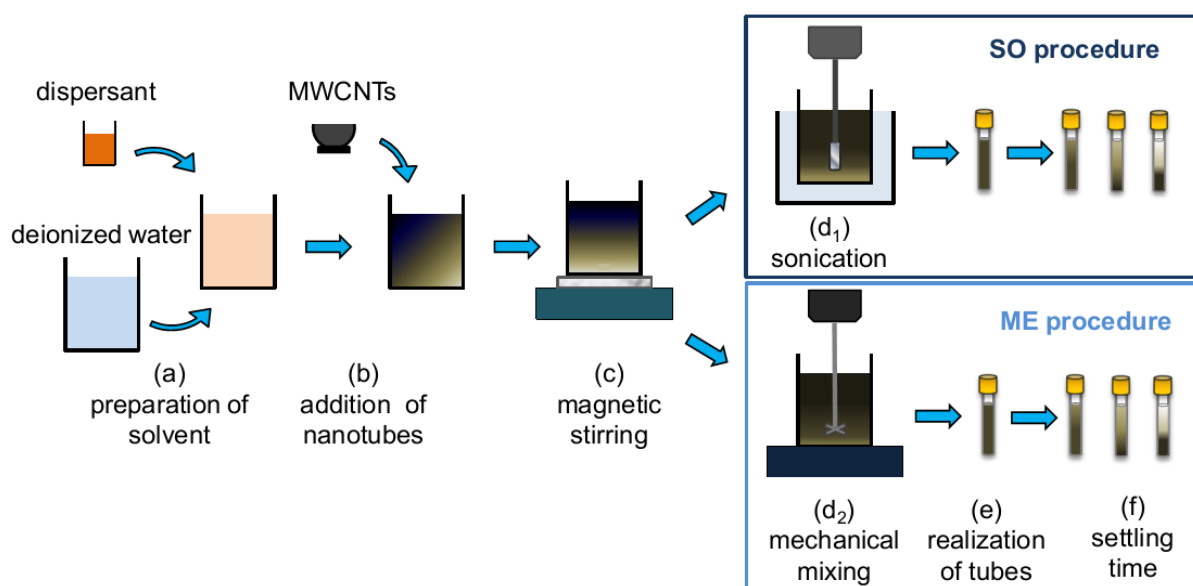


Figure 1 Considered preparation procedures, with and without sonication (SO and ME procedures, respectively), for dispersing MWCNTs in water.

3.4. Specimens' characteristics

Cement paste, mortar and concrete nanocomposite specimens were fabricated using different contents of MWCNTs and considering a selection of three dispersion procedures presented in the previous section.

Specimens were cubes of $5.1 \times 5.1 \times 5.1 \text{ cm}^3$ with embedded net-shaped electrodes. The embedded electrodes were stainless steel nets composed by 0.5 mm diameter wires, directly inserted in the specimens along approximately 85% of their thickness. In each specimen, five net electrodes, parallel to one face of the cube, were placed at mutual distances of 1 cm, which allowed making

measurements with different distances between electrodes. In the case of nanocomposite paste and mortar specimens, nets with a square mesh of 6 mm were used, while, in the case of nanocomposite concrete specimens, the embedded parts of the net electrodes were reduced to 4 wires having a distance of 12 mm, as depicted in Figure 2. The gross area of the embedded part of each electrode is approximately $4.3 \times 4.3 \text{ cm}^2$.

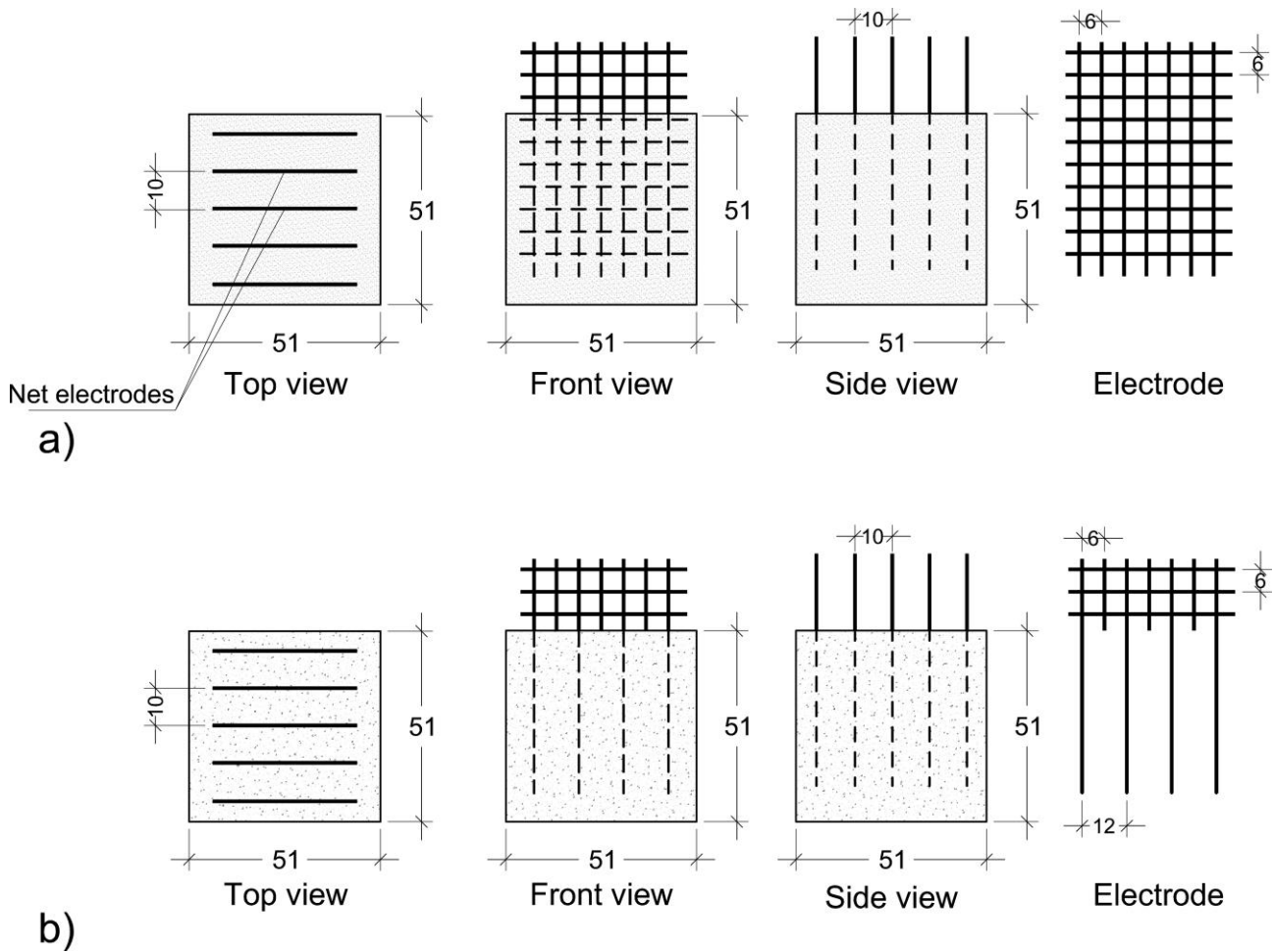


Figure 2 Sketch and dimensions (in mm) of fabricated nanocomposite cement-based specimens and electrodes: paste and mortar samples (a), concrete samples (b).

The composite specimens were named using the following identification code: "MT_MP_N%_DN_DR", where MT is the type of composite material, that can be paste (PA), mortar (MO) or concrete (CO), N% is the mass content of MWCNTs expressed as a percentage with respect to the mass of cement, while MP, DN and DR have the meaning defined in Section 3.3.

Six different concentrations of MWCNTs were considered, namely from 0 to 1% with respect to the mass of cement, with step increments of 0.25%, and from 1 to 1.5% with a step increment of 0.5%. Considering the three different types of composite materials, the three selected preparation procedures and the five different concentrations of MWCNTs, plus the three plain specimens, yields a total of $3 \times 3 \times 3 \times 5 = 48$ specimens. The mix designs of pastes, mortars and concretes, presented in Table 3, were chosen similar to those of typical cementitious materials used in constructions. The cement was pozzolanic, type 42.5. A second-generation plasticizer based on polycarboxylate ether polymers was added to the mixes in variable amounts, in order to obtain similar workability for all the mixes. In the mixes of mortars, aggregates were sand with nominal dimension from 0 to 4 mm, while, in the mixes of concretes, the same sand was complemented with gravel, having nominal dimension from 4 to 8 mm. Such coarse aggregates' dimensions were chosen taking into account the geometry of the specimens and of the electrodes.

The steps of the fabrication procedures of the specimens are detailed in Figure 3. First, an aqueous solution was prepared by adding dispersant to deionized water (Figure 3(a)). Then, carbon nanotubes were added (Figure 3(b)) by means of a preliminary mixing (Figure 3(c)) followed by a 30-minutes-long sonication or, alternatively, by a 60-minutes-long mechanical mixing (Figure 3(d)). After mixing the solution, cement powder, aggregates and plasticizer (Figure 3(e) and (f)) were added to obtain paste, mortar or concrete. Composite specimens were then stirred and poured into the molds (Figure 3(g)) and net electrodes were embedded (Figure 3(h)). After proper settling, the samples were unmolded for curing (Figure 3(i) and (j)). The specimens were cured for 28 days in controlled laboratory conditions.

For the sake of clarity, Table 4 summarizes the codes used in this paper to identify samples and specimens in dispersion and materials' characterization tests.

Table 3. Mix designs of fabricated cement-based composites with MWCNTs (C_0 is the mass of cement in plain cement-based materials, C is the mass of cement in cement-based composites, ΔV_{PA} , ΔV_{MO} and ΔV_{CO} represent the total volume of MWCNTs plus dispersant for composite paste, mortar and concrete, respectively, δ is the ratio between dispersant and MWCNTs mass and v is the ratio between MWCNTs and cement mass).

Components	Paste		Mortar		Concrete	
	Plain (kg/m ³)	Composite (kg/m ³)	Plain (kg/m ³)	Composite (kg/m ³)	Plain (kg/m ³)	Composite (kg/m ³)
Cement 42.5	$C_0 = 1277$	$C = C_0 \frac{1m^3}{1m^3 + \Delta V_{PA}}$	654	$C = C_0 \frac{1m^3}{1m^3 + \Delta V_{MO}}$	524	$C = C_0 \frac{1m^3}{1m^3 + \Delta V_{CO}}$
Water	574	0.45C	294	0.45C	234	0.45C
MWCNTs	-	vC	-	vC	-	vC
Dispersant	-	δvC	-	δvC	-	δvC
Sand (0-4mm)	-	-	1308	2C	951	1.81C
Gravel (4-8mm)	-	-	-	-	638	1.22C
Plasticizer	-	Var	-	Var	2.62	Var
Water/cement ratio	0.45	0.45	0.45	0.45	0.45	0.45

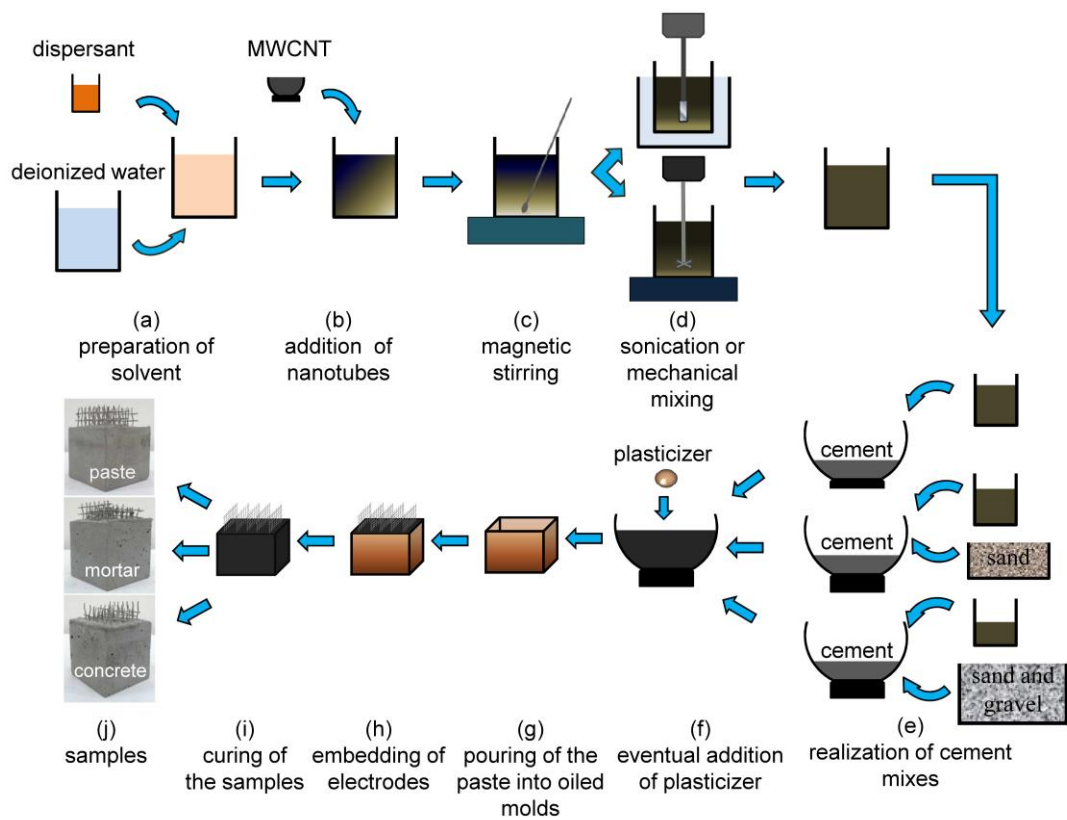


Figure 3 Preparation procedures of cement-based nanocomposite specimens (paste, mortar and concrete) using different mixing procedures (sonication or mechanical mixing)

Table 4. Sample and specimen identification codes used for the experiments.**Dispersion tests, sample identification code: "MP_DN_DR"**

Code	Variable	Value	Description
MP	Mixing procedure	SO	Sonicated
		ME	Mechanical
DN	Dispersant number	1,2,...,9	See Table 2
DR	Dispersant ratio	0.1:1	Ratio between dispersant and MWCNTs mass
		1:1	
		10:1	
		10:1(X) ^(*)	

Characterization tests, specimen identification code: "MT_MP_N%_DN_DR"

Code	Variable	Value	Description
MT	Material type	PA	Paste
		MO	Mortar
		CO	Concrete
N%	Mass content of MWCNTs	0-1.5%	Ratio between MWCNTs and cement mass

(*) For dispersant number 9 only (see Section 3.3)

4. EXPERIMENTAL METHODOLOGY

A campaign of experimental tests was carried out in order to systematically investigate the effectiveness of the considered procedures for fabricating carbon-nanotube-cement pastes, mortars and concretes. A first set of experiments, carried out at the Laboratory of Nanotechnology and Materials Science of the Department of Civil and Environmental Engineering of University of Perugia, was aimed at investigating the quality of the dispersion of MWCNTs in deionized water using the procedures described in Section 3.3. After identifying the best dispersing procedures, specimens made of composite cement paste, mortar and concrete were prepared and a second set of experiments was carried out to assess the quality of the composite materials by measuring their

electrical conductivity, its evolution in time and their percolation threshold. Finally, a third set of experiments was carried out at the Laboratory of Road Infrastructures, in order to assess the strain-sensitivity of the composites. In this section we present the experimental program for the three sets of experiments.

4.1 Analysis of the Quality of MWCNTs Dispersion

The quality of MWCNTs dispersion was investigated by both measuring the time of MWCNTs settling and by SEM inspections.

A classification of the different specimens based on a dispersion performance index, J , ranging from 0 to 6 was performed (0 corresponding to the worst dispersion and 6 to the best dispersion).

The dispersion index was computed as:

$$J = S_1 + S_{28} + P \quad (3)$$

where S_1 is called the "initial settling factor", S_{28} is called the "final settling factor" and P is called the "SEM picture factor".

S_1 and S_{28} factors derived from the analysis of test tubes containing 1 ml of the MWCNTs suspension diluted in 10 ml of deionized water (0.24 mg/ml of MWCNTs concentration). The initial settling factor, S_1 , was attributed a value of 0, 1 or 2 depending upon the assessment of the settling conditions of the suspension in the test tube after 1 day. A value $S_1 = 0$ corresponded to a situation where MWCNTs appeared to be completely separated from the water and were settled at the bottom of the test tube. The water above the settled MWCNTs was perfectly transparent as it was checked by taking a picture with a light beyond the test tube. A value $S_1 = 2$ corresponded to a situation where settling had not yet taken place and the suspension was black and fully opaque along the test tube. In this case, the picture with the light beyond the test tube was completely dark. The intermediate case ($S_1 = 1$) between these two extreme situations was identified when settling had partially taken place and, consequently, the thickness of the layer of settled MWCNTs was small

and a significant amount of suspended MWCNTs was revealed. In this case, the picture with the light beyond the test tube highlighted a semi-transparency of the suspension above the layer of settled MWCNTs.

The final settling factor, S_{28} , was attributed a value of 0, 1 or 2 following a procedure that was fully similar to the one adopted for S_1 , but carried out after 28 days. The basic idea was that a suspension that had not yet separated after 28 days indicated a better dispersion compared to one that had already separated.

The SEM picture factor was evaluated by analyzing SEM pictures of the specimens at different magnifications. For the SEM analysis a little drop of the obtained solutions was poured on a silicon wafer and the water was allowed to evaporate. A value $P = 0$ was assigned to the specimen when the picture showed bundles of MWCNTs already at the lowest magnification factor (100x). A value $P = 1$ was assigned to the specimen when the first bundles were visible at a magnification factor of 500x. A value $P = 2$ was assigned when the SEM image showed bundles at magnification factors greater than 5000x.

Figure 4 shows three typical pictures of retroilluminated test tubes corresponding to settling factors of 0, 1 and 2, as well as SEM images taken at different magnification factors elucidating situations corresponding to SEM picture factors of 0, 1 and 2.

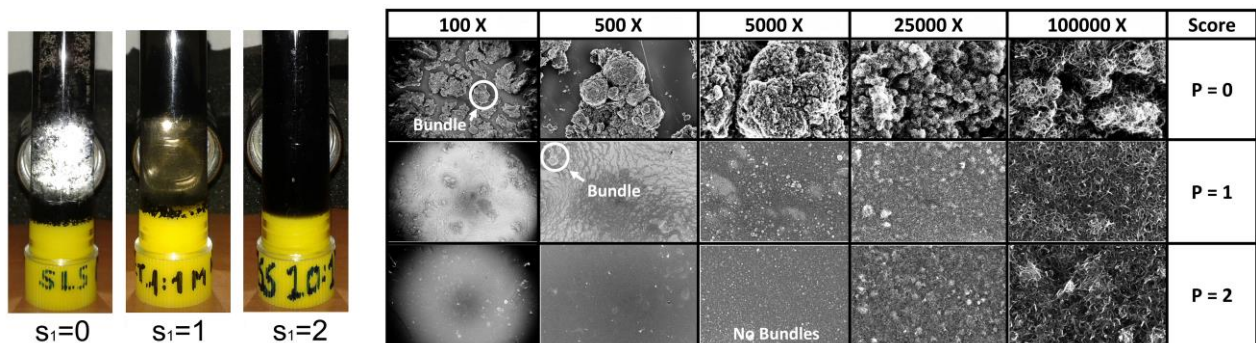


Figure 4 Illustrative samples corresponding to different initial settling factors (left) and to different SEM picture factors (right).

4.2 Electrical Characterization of the Composite Materials

Electrical characterization of the composite materials was carried out by two different experimental tests, one in DC current and the other one in AC current.

In the DC current test, a constant voltage difference, $V=1.5$ V, was applied at the two external electrodes, placed at a distance of 4 cm (see Figure 2), and the current, $I(t)$, circulating through the specimens was measured. The use of the two external electrodes for the measurements allowed to gain information on the electrical properties of the whole specimens. Because of polarization effects occurring in DC measurements, current intensity was not constant but was rather a function of time, t , that stabilized with increasing time. Measurements were taken with a high precision digital multimeter, model Keithley 6517B with resistivity test fixture model 8009, which also provides the stabilized potential difference to the specimens. Electrical resistance of the specimens was obtained by dividing the applied voltage by the measured current evaluated at a sufficiently large time instant, t_f , so as to practically attain the end of the polarization process. The DC-estimate of the electrical resistivity, ρ_{DC} , was thus obtained through multiplication of the electrical resistance by specimen's cross-section, A , and division by electrodes' distance, d , as follows:

$$\rho_{DC} = \frac{V}{I(t)|_{t=t_f}} \frac{A}{d} \quad (4)$$

A value of t_f equal to 3 minutes was used in the experiments.

In the AC test, the AC-estimate of the electrical resistivity of the composites, ρ_{AC} , was obtained by measuring the electrical resistance of the specimens, $R_{AC}(\omega)$, through a high precision LCR meter, model HM8018. The following relation was applied to obtain ρ_{AC} :

$$\rho_{AC} = R_{AC}(\omega)|_{\omega=\bar{\omega}} \frac{A}{d} \quad (5)$$

where ω is the AC frequency, chosen equal to the maximum value allowed by the instrument: $\bar{\omega} = 25\text{kHz}$. The main advantage of the AC measurement is that it eliminates the effects of polarization. For each specimen, the AC test was carried out for all four pairs of electrodes placed at a distance of 1 cm so as to obtain information on data scatter within the same specimens, which is related to the quality of nanotubes' dispersion and to its homogeneity in space.

For convenience, results of both DC and AC electrical characterization tests are expressed in terms of electrical conductivity, which is more commonly used in the literature in comparison to electrical resistivity, where conductivity is obtained as the inverse of the resistivity computed by Eq. (4) or by Eq. (5).

4.3 Assessment of Strain-Sensing Property of the Composite Materials

Axial compression tests were carried out to assess the strain-sensing capability of the composite materials. The testing equipment was a servo-controlled pneumatic universal testing machine, model IPC Global UTM14P, having 14 kN load capacity (see Figure 5). The sensing specimens were subjected to loading-unloading cycles at constant, low, speed and amplitudes varying from about 0.2 to 0.8 MPa (see Figure 6). Average compressive strain in the composites was obtained by using two electric strain gauges mounted on opposite faces of the specimens, while strain sensitivity, S , Eq. (2), was obtained by measuring ΔR through a data acquisition system. Similarly to the electrical characterization tests, the two probe method was used, which allowed to be consistent with previous results by the authors [29-31] and to use coaxial cables for reducing measurement noise even at high sampling rates.

Two active electrodes placed at a distance of 1 cm were considered for the measurements in each specimen, achieving, in this way, good signal to noise ratios with low voltage. The data acquisition system was a high speed digital multimeter (National Instruments (NI) PXI4071) installed into a NI PXIe1073 that also hosted a source measure unit, model NI PXI4130, providing a stabilized potential difference of 1.5 V in a single isolated channel and a data acquisition card, model NI PXIe-4330, for strain gauges. Strain gauges were 2 cm long, had a nominal resistance of 120 Ω and a gauge factor of about 2. Strain-induced incremental variation in electrical resistance, $\Delta R(t)$, was obtained by dividing the applied voltage, V , by the incremental variation in measured current intensity, $\Delta I(t)$. By introducing $\Delta R(t)$ into Eq. (1), the following equation is obtained for strain estimation:

$$\varepsilon(t) = -\frac{V}{\lambda R_0 \Delta I(t)} \quad (6)$$

The gauge factor, λ , in Eq. (6) was estimated by best fitting of strain measured with strain gauges and strain estimated from Eq. (6). The sampling time for current and strain measurements was chosen equal to 0.015 s.

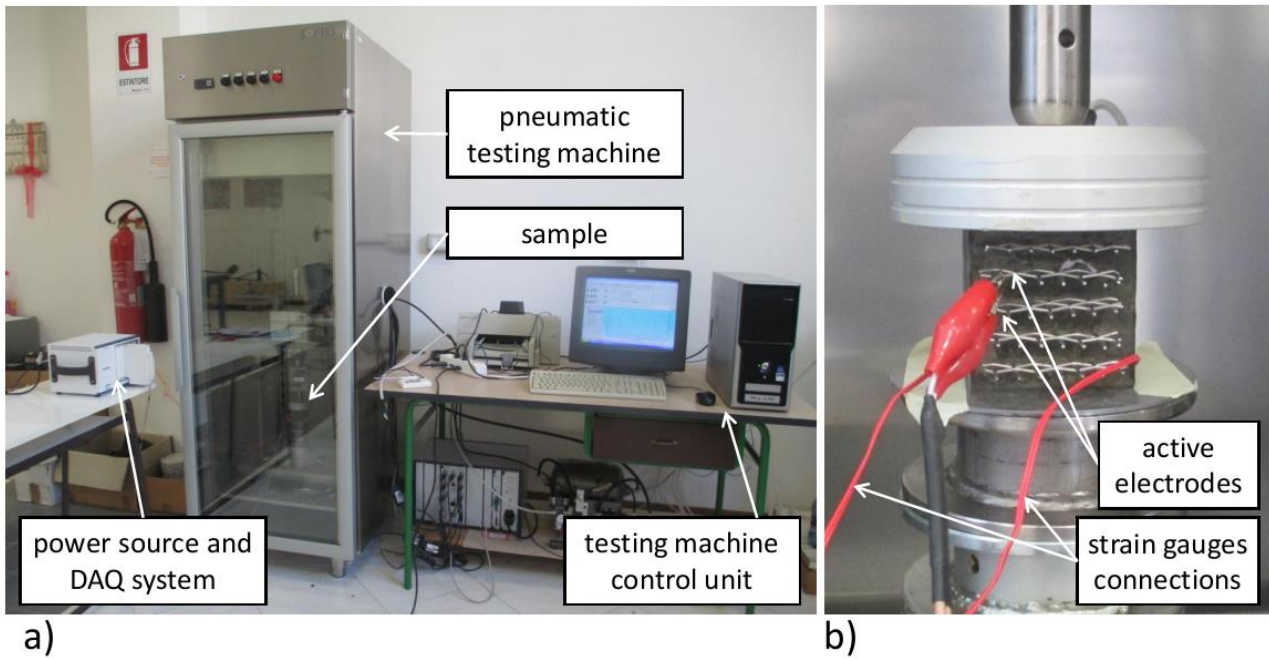


Figure 5 a) Test set-up for strain sensing assessment of the composite materials; b) detailed view of coaxial cables connected to the net electrodes of the sample.

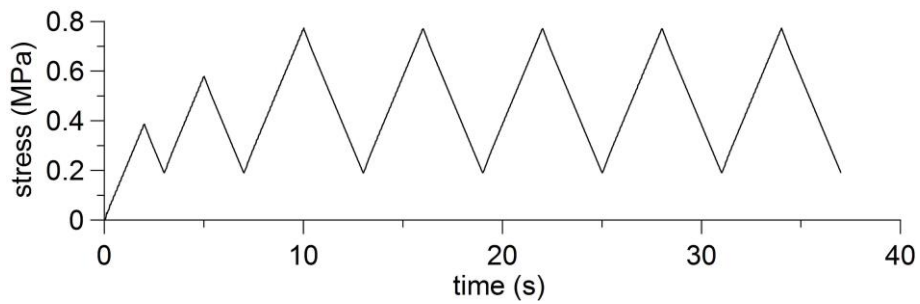


Figure 6 Time history of applied compression stress in strain sensing tests

5. RESULTS AND DISCUSSION

5.1. Dispersion

Figure 7 shows the scores obtained by the different specimens in MWCNTs dispersion tests, computed according to Eq. (3) and considering only specimens corresponding to scores greater than zero. The results show that sonication systematically determines an improvement in dispersion that is evidenced by the larger performance indexes in comparison to the cases with mechanical mixing. Mechanical mixing always yields poor quality of dispersion ($J \leq 3$) with the only significant exception of dispersant number 6 (SLS) that, used in the amount of 10:1, provides a very good score ($J=4$) even with mechanical mixing (specimen ME_6_10_1 in Figure 7). In this case, although bundles appear at 100X magnification factor ($P=0$), the MWCNTs water suspension remains stable even after 28 days. Therefore, the dispersion can be considered as satisfactory, but electrical and strain sensing tests are necessary to investigate the possible detrimental effects of MWCNTs bundles on the quality of the composites.

Type and amount of dispersant are also seen to be crucial for achieving a good dispersion. In particular, no specimen with 0.1:1 concentration of dispersant has qualified for a score greater than zero and specimens with 10:1 concentration mostly attain scores that are greater than those obtained by specimens with 1:1 concentrations. As notable exceptions, excellent performances of dispersants number 3 (DISPERBYK190) and 6 (SLS) are evidenced, that, when sonicated, attain the top score already with a 1:1 concentration. When sonicated and used in the 10:1 concentration, all types of dispersants provide very good results ($J \geq 4$). The poor dispersion of CNTs in water using dispersant number 8 (PVA) is probably due to the presence of hydrophilic groups in the macromolecule that does not promote a good compatibility between the hydrophobic surface of nanotubes and the solvent.

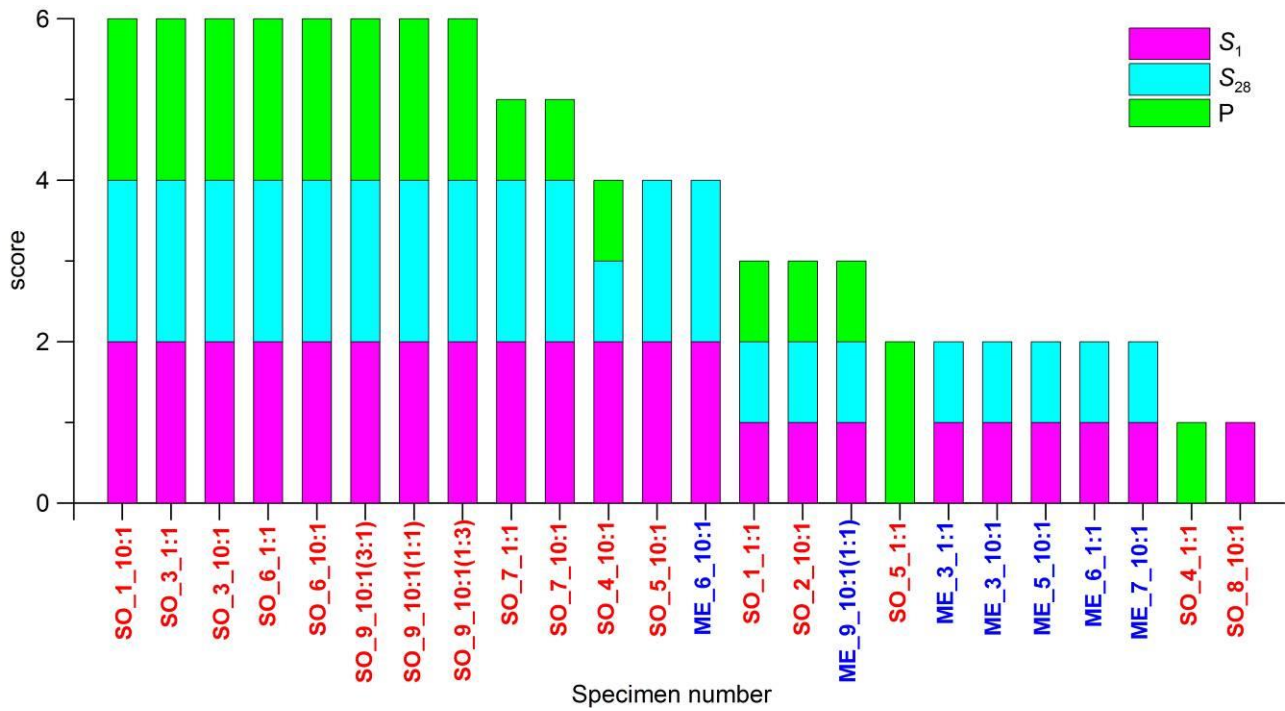


Figure 7 Scores obtained by different specimens in MWCNTs dispersion tests using Eq. (3) (specimens with zero score are omitted, specimens identification codes are defined in Table 4, sonicated specimens are indicated in red, mechanically mixed specimens are indicated in blue)



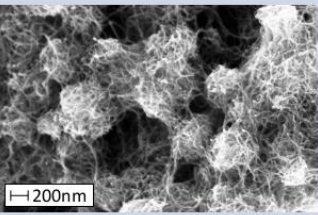


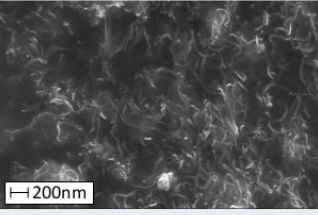


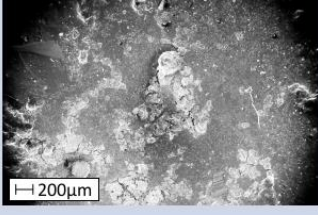
Sample identification	Initial settl. factor S_1	Final settl. factor S_{28}	SEM picture factor P	Final Score
SO_6_1:1	 $S_1 = 2$	 $S_{28} = 2$	 $P = 2$	6
SO_6_10:1	 $S_1 = 2$	 $S_{28} = 2$	 $P = 2$	6
ME_6_10:1	 $S_1 = 2$	 $S_{28} = 2$	 $P = 0$	4

Figure 8 Scores obtained by the three selected procedures for dispersing nanotubes using Eq. (3) (samples identification codes are defined in Table 4): sonicated specimens using the SLS dispersant in the 1:1 (SO_6_1:1) and 10:1 (SO_6_10:1) amounts and mechanically mixed specimen using the SLS dispersant in the 10:1 amount (ME_6_10:1)

In light of the results presented above, it was decided to prepare sonicated specimens using the SLS dispersant in the 1:1 and 10:1 amounts and mechanically mixed specimens using the same dispersant in the 10:1 amount (see Figure 8). Considering the three selected combinations for dispersing nanotubes, the five different MWCNTs concentrations and the three different types of composite material (pastes, mortars and concretes), a total of $3 \times 5 \times 3 = 45$ specimens were manufactured, with the addition of three control specimens (plain paste, mortar and concrete).

5.2. Percolation

Figure 9 shows the evolution of the DC-measured electrical conductivity of the fabricated composite specimens versus curing time. The results highlight that there is a general trend of decreasing electrical conductivity in time which is more apparent in composites with low contents of MWCNTs. This effect is associated with the loss of water, due to drying and absorption caused by cement hydration, and consequent loss of ionic conduction. The presence of a significant amount of MWCNTs, above the percolation threshold, determines the formation of a primary conduction path, through the nanotubes, that reduces the relative contribution of ionic conduction to the overall composites' conductivity, thus mitigating conductivity evolution with curing time.

The results of Figure 9 also show an almost consistent increment in conductivity with MWCNTs content. Incorporation of MWCNTs determines an increase in conductivity up to about two orders of magnitude with respect to plain materials. This result, as well as obtained values of conductivity of plain cement-based materials, are in line with other literature results [23].

The effect of MWCNTs content on composites' electrical conductivity is investigated in more details in Figure 10 showing the results of AC electrical characterization tests carried out on cured specimens. The results show a clear percolation threshold around 1% of MWCNTs content for composite concrete specimens, with similar values of conductivity for sonicated and mechanically mixed specimens. Percolation is also identified around 1% of MWCNTs content for sonicated and mechanically mixed mortar with 10:1 concentration of dispersant, which might be explained by the

similar mixes of mortars and concretes (see Table 3). On the contrary, the use of a 1:1 concentration of dispersant in the mortar is seen to lead to unsatisfactory results for contents of MWCNTs greater than 0.8%, which indicates that the presence of fine aggregates reduces the effectiveness of the SLS dispersant, conceivably because of excessive water and dispersant absorption by aggregates themselves. Percolation is instead less clearly identifiable in composite paste specimens, because MWCNTs contribution to electrical conductivity is marginal in this case and because, differently from the percolation response of mortars and concretes, double percolation phenomena [57] do not take place in paste specimens.

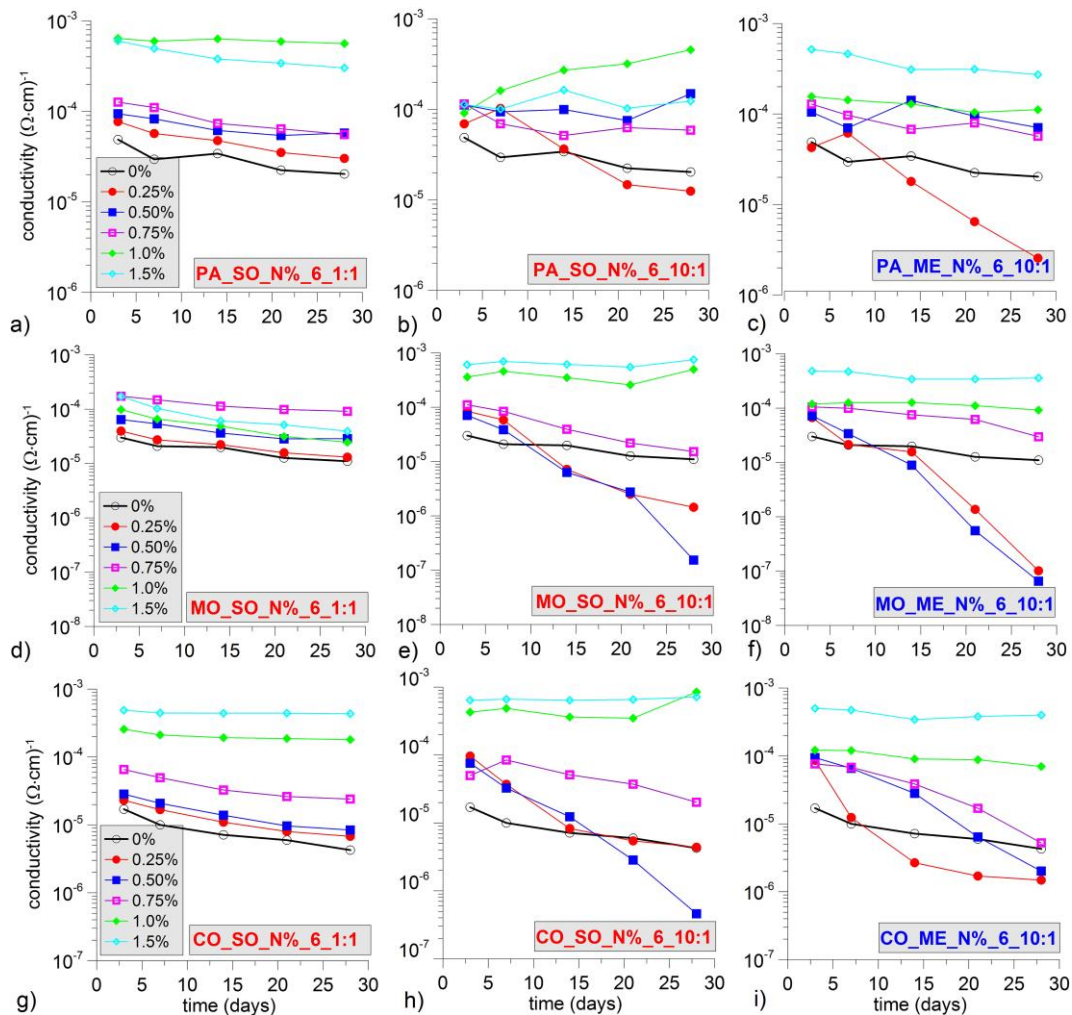


Figure 9 Evolution of composites' electrical conductivity with curing time considering different preparation strategies and different mass contents of MWCNTs expressed as a percentage with respect to the mass of cement, in DC electrical characterization tests (specimens identification codes are defined in Table 4): composite pastes (a, b, c); composite mortars (d, e, f); composite concretes (g, h, i).

Results presented in Figure 10 also evidence that the use of a relatively large quantity of SLS dispersant (10:1 concentration), in combination with a small amount of MWCNTs, is associated with a decrease in electrical conductivity with respect to the plain material. It is hypothesized that this circumstance is caused by the formation of a partially isolating coating, perhaps an electrochemical double-layer (polarization resistance) [34], on the surface of the nanotubes, so that nanotubes behave as non-conductive inclusions when they are in the dilute regime, that is, when their mutual distances are high. When the content of nanotubes is increased, and their mutual distances are decreased, this effect is canceled and nanotubes interactions dominate the electrical conductivity of the composite.

By computing the ratio between the electrical conductivity of the composites and the electrical conductivity of the corresponding plain cement-based materials, considering a content of MWCNTs equal to 1.5%, it is revealed that relative increase in electrical conductivity grows when ranging from paste to mortar and concrete. In particular, this ratio for pastes is equal to 12 (PA_SO_1.5%_6_1:1), 29 (PA_SO_1.5%_6_10:1) and 45 (PA_ME_1.5%_6_10:1), for mortars is equal to 6 (MO_SO_1.5%_6_1:1), 112 (MO_SO_1.5%_6_10:1) and 68 (MO_ME_1.5%_6_10:1) and for concretes is equal to 93 (CO_SO_1.5%_6_1:1), 262 (CO_SO_1.5%_6_10:1), 127 (CO_ME_1.5%_6_10:1). The observed trend is due to the circumstance that aggregates reduce the electrical conductivity of the plain materials, while they are almost ineffective above the percolation threshold due to the formation of a conductive network of nanotubes. The only exception to this trend is represented by the mortar sonicated with 1:1 concentration of dispersant, that, as already commented above, is not significant due to an insufficient quality of the material.

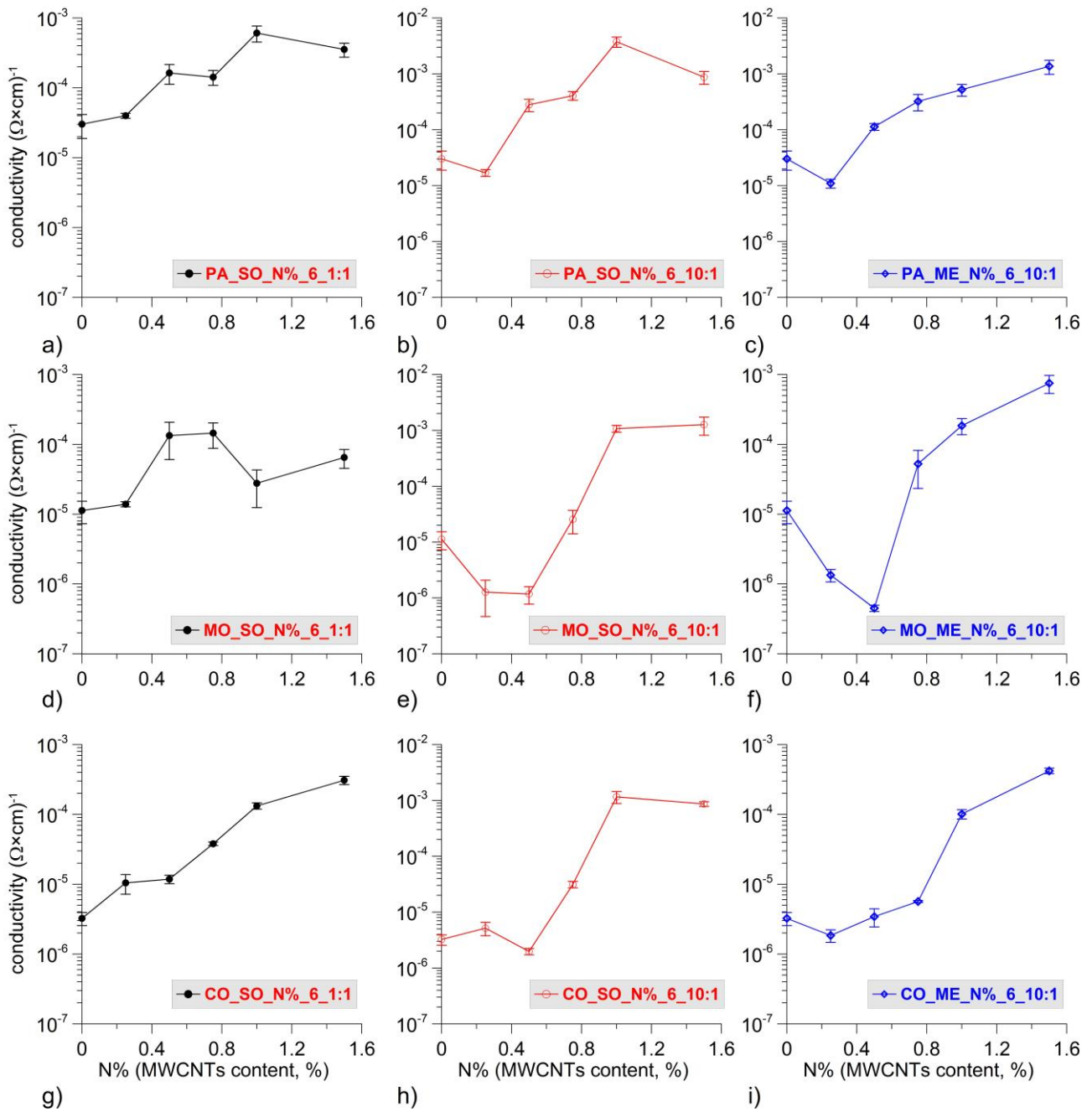


Figure 10 Electrical conductivity of composite specimens versus MWCNTs mass content expressed as a percentage with respect to the mass of cement, in AC electrical characterization tests (specimens identification codes are defined in Table 4, the error bars denote \pm standard deviation intervals, with standard deviations computed by varying distance between electrodes): composite pastes (a, b, c); composite mortars (d, e, f); composite concretes (g, h, i)

5.3. Sensing

Strain sensing tests have been performed by imposing to the specimens a compression load with the time history already presented in Figure 6. Specimens close to the percolation threshold have been

chosen for the tests, as they are those for which the best strain sensing capabilities are expected. For all specimens, except for sonicated mortar with 1:1 dispersant concentration, the chosen amount of MWCNTs is the 1.0% with respect to the weight of cement. In the case of mortar, specimen MO_SO_1.0_6_1:1 is discarded because of its low electrical conductivity (cfr. Section 5.2) and substituted by specimen MO_SO_0.75_6_1:1 which better approximates percolation.

Information on gauge factor, λ , Eq. (1), and strain sensitivity, S , Eq. (2), obtained from tests results is reported in Table 5. The table also reports information on the amplitudes of the incremental variations in current intensity, electrical resistance and axial strain, denoted as ΔI , ΔR and $\Delta \epsilon$, respectively, under compression loading cycles ranging from 0.2 to 0.8 MPa, as well as on the root mean square of the noise in current measurements, denoted as ϵ_I . The ratio between ΔI and ϵ_I is the signal to noise ratio of the measurements, indicated as SNR.

The time histories of the strain measured with strain gauges and of the strain estimated from current measurements, using Eq. (5), are depicted in Figure 11. From these results, it is apparent that the incremental variations in strain are correctly estimated with all composite specimens, but the slow time variations of electrical resistance associated with different levels of electrical polarization can sometimes impede the estimation of the absolute value of the strain. This is an issue that could be resolved by an improved measurement hardware, notably a dedicated electronics, whose investigation goes however beyond the purposes of this paper.

The results of the axial compression tests demonstrate the strain sensing ability of the composites and highlight that mechanically mixed specimens have larger sensitivity and larger values of the gauge factor compared to sonicated specimens. The obtained values of the gauge factor of mechanically mixed specimens compare well with other literature studies on sonicated composites, showing larger gauge factors for pastes [25], in comparison to mortars and concretes [49].

Concerning the quality of the output signals in terms of SNR, the results summarized in Table 5 show that this reduces slightly from sonicated to mechanically mixed specimens, while it decreases more drastically from pastes to mortars and concretes, due to a decrease in gauge factor. In this

regard, Figure 12 shows a comparison between the electrical outputs of sonicated and mechanically mixed specimens, highlighting the similarity of the signals outputted by composite paste specimens, while evidencing some loss in signal quality in the case of mechanically mixed composite mortar and concrete specimens in comparison with sonicated ones.

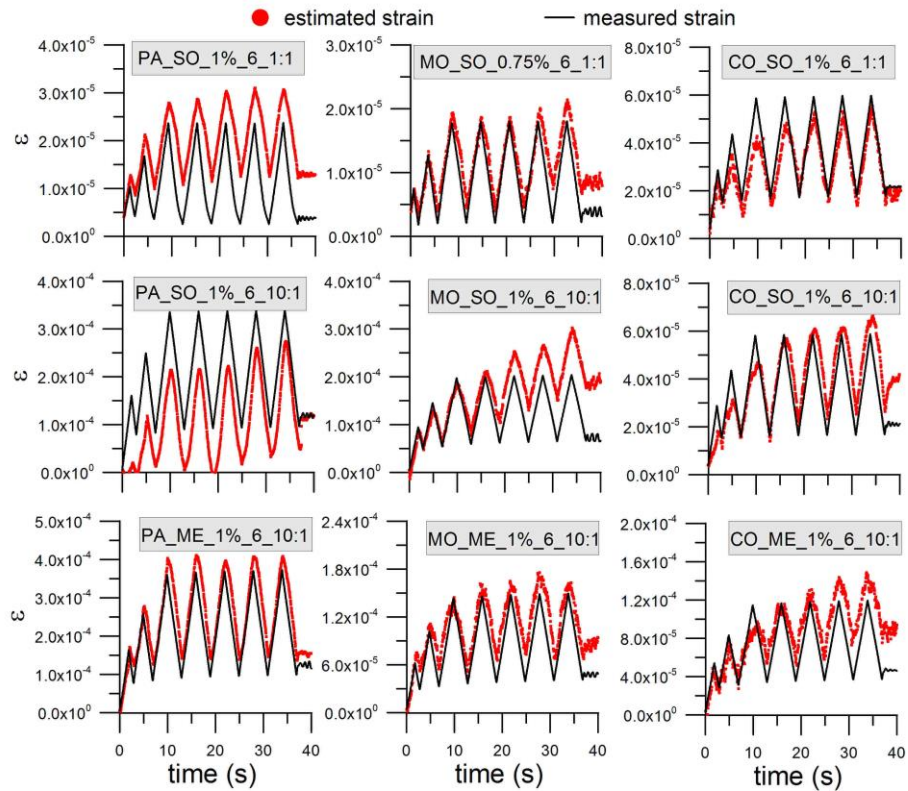


Figure 11 Time-histories of measured and estimated strain for paste, mortar and concrete composite specimens

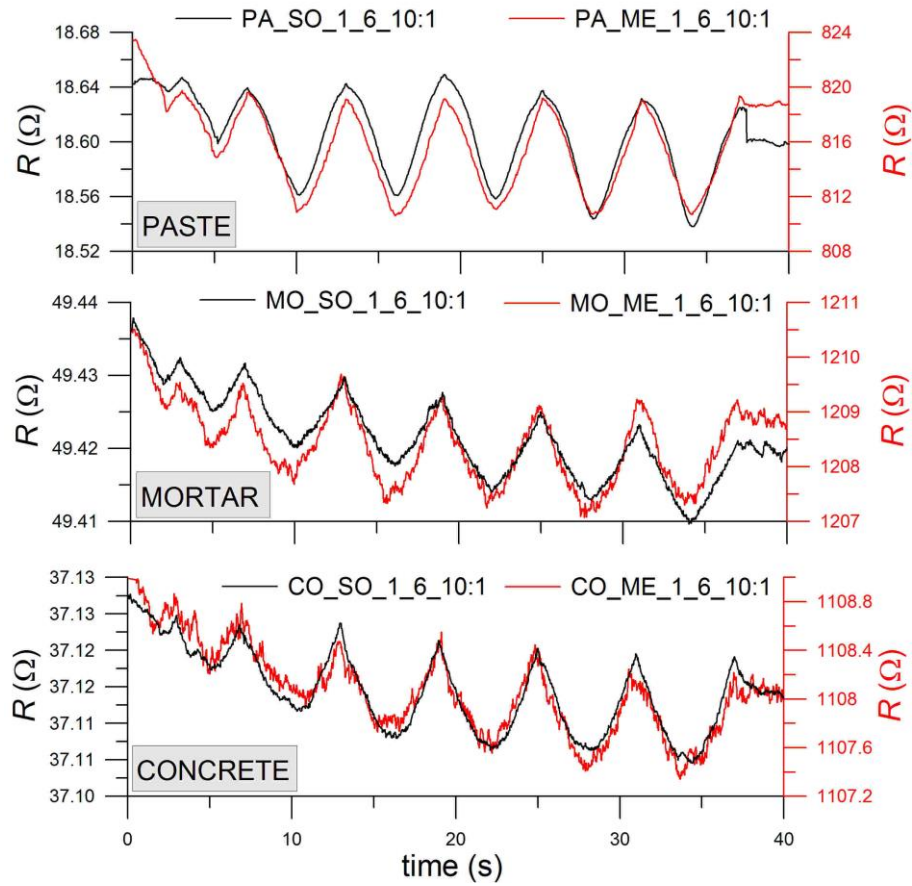


Figure 12 Time-histories of electrical resistance under axial loading (Figure 6) for sonicated and mechanically mixed composite specimens of paste (PA_SO_1_6_10:1 and PA_ME_1_6_10:1), mortar (MO_SO_1_6_10:1 and MO_ME_1_6_10:1) and concrete (CO_SO_1_6_10:1 and CO_ME_1_6_10:1).

Table 5. Results of strain sensing tests (ΔI , ΔR and $\Delta \varepsilon$ are variations in current intensity, electrical resistance and axial strain, respectively, under a compression loading cycle ranging from 0.2 to 0.8 MPa; ε_I is the standard deviation of the noise in current measurements and $SNR = \Delta I / \varepsilon_I$ is the signal to noise ratio)

Specimen	ΔI (mA)	ε_I (μ A)	SNR	ΔR (Ω)	$\Delta \varepsilon$	λ	S (Ω)
PA_SO_1_6_1:1	0.015	0.124	119	0.254	2.13e-5	80	11940
PA_SO_1_6_10:1	0.412	3.839	107	0.095	2.45e-4	21	387
PA_ME_1_6_10:1	0.020	0.178	111	8.740	2.76e-4	130	31635
MO_SO_0.75_6_1:1	0.001	0.036	19	0.166	1.59e-5	25	10428
MO_SO_1_6_10:1	0.008	0.276	28	0.013	1.40e-4	2	89
MO_ME_1_6_10:1	0.002	0.202	11	2.195	1.10e-4	68	19861
CO_SO_1_6_1:1	0.001	0.053	24	0.095	4.24e-5	7	2235
CO_SO_1_6_10:1	0.017	0.523	32	0.015	4.23e-5	10	365
CO_ME_1_6_10:1	0.001	0.087	14	0.992	8.35e-5	23	11879

6. CONCLUSIONS

This paper reports an experimental investigation of the effects of different preparation strategies over electrical conductivity, percolation and strain-sensing properties of cement-based composites. The aim of this study is the identification of a suitable scalable preparation strategy, compatible with large-scale deployment of multifunctional self-sensing cement-based composites for structural health monitoring of civil constructions.

The experiments have focused on cement paste, mortar and concrete composites doped with multi-walled carbon nanotubes. The proper dispersion of nanotubes in water, prior to the addition of cement powder and aggregates, is identified as the key preparation issue and the bottleneck limiting scalability of self-sensing composites to full-scale structures. Therefore, different strategies have been considered to achieve such a dispersion, whose quality has been evaluated by means of an objective procedure. More specifically, the quality of dispersion has been judged on the basis of the rate of separation of the nanotubes from the water and on the basis of the minimum magnification factor necessary to clearly detect the presence of MWCNTs bundles using scanning electron microscopy. Considered preparation strategies are either based on mechanical mixing procedures or on the more complicated sonic treatment and also envisage the possible use of different dispersing additives in different concentrations.

The results have demonstrated the superior quality of the dispersion obtained when carrying out the sonic treatment and the crucial role played by type and concentration of dispersing additive. The best dispersant has been identified as the one yielding: (i) an optimal dispersion of nanotubes when used in a relatively low concentration and combined with sonication and (ii) a fairly good dispersion when used in a higher concentration without sonication, with stable MWCNTs water suspensions even if affected by local bundles. Based on these findings, specimens of cement pastes, mortars and concretes with different concentrations of MWCNTs have been prepared using three preparation strategies. The first preparation strategy consists of using the best dispersing additive without sonication and is identified as the "scalable procedure". The remaining two strategies

consider the same additive, at similar and lower concentrations, and also include the sonic treatment.

The fabricated specimens have been subjected to experimental tests with the purpose of measuring their electrical conductivity, also investigating its variation with curing time and content of nanotubes, and of assessing their strain-sensing properties. The results have highlighted the effectiveness of the scalable procedure that is seen to provide composites that, despite the presence of MWCNTs bundles in water suspensions, exhibit very similar percolation thresholds (around 1% of MWCNTs with respect to the weight of cement), electrical conductivity (around $5.2\text{E-}4$, $1.8\text{E-}4$ and $1.0\text{E-}4$ $(\Omega\text{cm})^{-1}$ for pastes, mortars and concretes, respectively) and strain-sensitivity (with gauge factors equal to 130, 68 and 23 for pastes, mortars and concretes, respectively) compared to sonicated composites. This fabrication procedure might be therefore potentially suitable for casting full-scale self-sensing structural components and for large-scale deployment of self-sensing cement-based materials and deserves further research regarding other relevant aspects whose consideration goes beyond the purposes of the present paper. Among those aspects, it will be worth studying more closely the repeatability and reliability of specimens' properties and, primarily, of the gauge factor, that should be investigated by testing a large number of nominally similar specimens with same concentration of nanotubes, as well studying linearity and quality of output signal.

ACKNOWLEDGEMENTS

This research was partially supported by Regione Umbria, within POR Umbria ESF 2007–2013, Axis II "Employability" Objective "e" Axis IV "Human Capital" Objective "I".

REFERENCES

1. J.M.W. Brownjohn, Structural health monitoring of civil infrastructure, Philos T. R. Soc. A 365(1851) (2007) 589-622.
2. U.S. Department of Transportation, Report to Congress - Technical Report, 2008.
3. V. Mosquera, A.W. Smyth, R. Betti, Rapid Evaluation and Damage Assessment of Instrumented Highway Bridges, Earthq. Eng. Struc. 41(4) (2012) 755-774.

4. X. Zhou, L. Xi, J. Lee, Reliability-centered predictive maintenance scheduling for a continuously monitored system subject to degradation, *Rel. Eng. Syst. Saf.* 92(4) (2007) 530-534.
5. F. Magalhaes, A. Cunha, E. Caetano, Vibration based structural health monitoring of an arch bridge: From automated OMA to damage detection, *Mech. Syst. Sig. Proc.* 28 (2012) 212-228.
6. M. Liu, D.M. Frangopol, K. Kwon, Fatigue reliability assessment of retrofitted steel bridges integrating monitoring data, *Struct. Saf.* 32(1) (2010) 77-89.
7. B. F. Spencer Jr, M.E. Ruiz-Sandoval, N. Kurata. Smart sensing technology: opportunities and challenges, *Struct. Control Health Monit.* 11 (2004) 349-368.
8. B. Han, X. Yu, E. Kwon, A self-sensing carbon nanotube/cement for traffic monitoring, *Nanotechnology* 20 (2009) 5pp.
9. B. Han, Y. Wang, S. Dong, L. Zhang, S. Ding, X. Yu, J. Ou, Smart concretes and structures: A review, *J. Intell. Mater. Syst. Struct.* 26 (11) (2005) 1303-1345
10. X. Yu, E. Kwon, A carbon nanotube/cement composite with piezoresistive properties, *Smart Mater. Struct.* 18 (2009) 5pp.
11. T.C. Hou, J.P. Lynch, Conductivity-based strain monitoring and damage characterization of fiber reinforced cementitious structural components, *Proc. SPIE, The International Society for Optical Engineering* 5765 (PART 1) 44 (2005) 419-429
12. J. Luo, Z. Duan, T. Zhao, Q. Li, Hybrid effect of carbon fiber on piezoresistivity of carbon nanotube cement-based composite, *Adv. Mat. Res.* 143-144 (2011) 639-643
13. M.S. Konsta-Gdoutos and C.A. Aza, Self sensing carbon nanotube (CNT) and nanofiber (CNF) cementitious composites for real time damage assessment in smart structures, *Cem. Conc. Comp.* 53 (2014) 110-128
14. Z.H. Zhu, Piezoresistive strain sensors based on carbon nanotube networks: Contemporary approaches related to electrical conductivity, *IEEE Nanotechnology Magazine* 9 (2) (2015) 11-23
15. H. Li, H. Xiao, J. Ou, A study on mechanical and pressure-sensitive properties of cement mortar with nanophase materials, *Cem. Concr. Res.* 34 (2003) 435-438.
16. S. Wen, D.D.L. Chung, Model of piezoresistivity in carbon fiber cement, *Cem. Concr. Res.* 36 (2006) 1879-1885.
17. O. Galao, F.J. Baeza, E. Zornoza, P. Garcés, Strain and damage sensing properties on multifunctional cement composites with CNF admixture, *Cem. Concr. Comp.* 46 (2014) 90-98
18. S. Laflamme, F. Ubertini, H. Saleem, A. D'Alessandro, A. Downey, H. Ceylan, A.L. Materazzi, Dynamic Characterization of a Soft Elastomeric Capacitor for Structural Health Monitoring, *J. Struct. Eng.*, in press available online, doi:10.1061/(ASCE)ST.1943-541X.0001151, 04014186 (2014)

19. L. Chiacchiarelli, M. Rallini, M. Monti, D. Puglia, J.M. Kenny, L. Torre, The role of irreversible and reversible phenomena in the piezoresistive behavior of graphene epoxy nanocomposites applied to structural health monitoring, *Compos. Sci. Technol.* 80 (2013) 73–79
20. M. Monti, M. Natali, J.M. Kenny, L. Torre, Carbon nanofibers for strain and impact damage sensing in glass fiber reinforced composites based on an unsaturated polyester resin, *Polym. Compos.* 32(5) (2011) 766-775
21. P. Mondal, S.P. Shah, L.D. Marks, Nanoscale characterization of cementitious materials, *ACI Mat. J.* 105 (2008) 174-179.
22. S.P. Shah, M.S. Konsta-Gdoutos, Z.S. Metexa, P. Mondal, Nanoscale Modification of Cementitious Materials, In: *Nanotechnology in Construction 3*, edited by Z. Bittnar et al, Springer, 2009, pp 125-130.
23. J. Cao, D.D.L. Chung, Electric polarization and depolarization in cement-based materials, studied by apparent electrical resistance measurement, *Cem. Concr. Res.* 34 (2004) 481-485
24. S. Wen, D.D.L. Chung, Damage monitoring of cement paste by electrical resistance measurement, *Cem. Concr. Res.* 30 (2000) 1979-1982
25. F. Azhari, N. Banthia, Cement-based sensors with carbon fibers and carbon nanotubes for piezoresistive sensing, *Cem. Concr. Comp.* 34 (2012) 866-73
26. B. Han, J. Ou, Embedded piezoresistive cement-based stress/strain sensors, *Sensor Actuat. A - Phys.* 138 (2007) 294-298
27. S. Wen, D.D.L. Chung, Partial Replacement of Carbon Fiber by Carbon Black in Multifunctional Cement-Matrix Composites, *Carbon* 45(3) (2007) 505-513
28. A.L. Materazzi, F. Ubertini, A. D'Alessandro, Carbon nanotube cement-based transducers for dynamic sensing of strain, *Cem. Conc. Comp.* 37 (2013) 2-11
29. F. Ubertini, S. Laflamme, H. Ceylan, A.L. Materazzi, G. Cerni, H. Saleem, A. D'Alessandro, A. Corradini, Novel Nanocomposite Technologies for Dynamic Monitoring of Structures: a Comparison between Cement-Based Embeddable and Soft Elastomeric Surface Sensors, *Smart Mater. Struct* 23(4) (2014) 12pp
30. F. Ubertini, A.L. Materazzi, A. D'Alessandro, S. Laflamme, Natural frequencies identification of a reinforced concrete beam using carbon nano tube cement-based sensors, *Eng. Struct.* 60 (2014) 265-275
31. A. D'Alessandro, F. Ubertini, A.L. Materazzi, M. Porfiri, S. Laflamme, Electromechanical Modelling of New Nanocomposite Carbon Cement-based Sensors for Structural Health Monitoring, *Struct. Heal. Monit.*, in press available online, doi:10.1177/1475921714560071 (2014)
32. G.Y. Li, P.M. Wang, X. Zhao, Pressure-sensitive properties and microstructure of carbon nanotube reinforced cement composites, *Cem. Concr. Comp.* 29 (2007) 377-382

33. H. Li, H. Xiao, J. Ou, Effect of compressive strain on electrical resistivity of carbon black-filled cement-based composites, *Cem. Concr. Comp.* 28 (2006) 824-828
34. S. Wansom, N.J. Kidner, L.Y. Woo, T.O. Mason, AC-impedance response of multi-walled carbon nanotube/cement composites, *Cem. Concr. Comp.* 28 (2006) 509-519
35. C. Rainieri, Y. Song, G. Fabbrocino, J.S. Mark, V. Shanov. CNT-cement based composites: Fabrication, self-sensing properties and prospective applications to Structural Health Monitoring, *Proc. SPIE, Fourth International Conference on Smart Materials and Nanotechnology in Engineering* 8793 (2013) 10 pp.
36. O. Lourie, D.E. Wagner, Buckling and collapse of embedded carbon nanotube, *Phys. rev. Lett.* 81(8) (1998) 1638-1641
37. S. Chuah, Z. Pan, J.G. Sanjayan, C.M. Wang, W.H. Duan, Nano reinforced cement and concrete composites and new perspective from graphene oxide, *Constr. Build. Mater.* 73 (2014) 113-124
38. B. Han, X. Yu, J. Ou, *Self-sensing concrete in smart structures*. Butterworth-Heinemann, Elsevier, 2014
39. M.S. Konsta-Gdoutos, Z.S. Metexa, S.P. Shah, Highly dispersed carbon nanotube reinforced cement-based materials, *Cem. Concr. Res.* 40(7) (2010) 1052-1059
40. P. Xie, P. Gu, J.J. Beaudoin, Electrical percolation phenomena in cement composites containing conductive fibers, *J. Mater. Sci.* 31 4093-4097 (1996)
41. S. Wen, D.D.L. Chung, Double percolation in the electrical conduction in carbon fiber reinforced cement-based materials, *Carbon* 45 (2007) 263-267
42. F. Ko, Y. Gogotsi, A. Ali, N. Naguib, H. Ye, G.L. Yang, C. Li, P. Willis, Electrospinning of continuous carbon nanotube-filled nanofiber yarns. *Adv. Mater.* 15 (2003) 1161–1165
43. J. Makar, J. Beaudoin, Carbon nanotubes and their application in the construction industry. In: P. Bartos, et al., eds. *Proceedings of the 1st international symposium on nanotechnology in construction (NICOM 2003)*, 331–341
44. C. Thauvin, S. Rickling, P. Schultz, H. Céilia, S. Meunier, C. Mioskowski, Carbon nanotubes as templates for polymerized lipid assemblies. *Nature Nanotechnology* 3 (2008) 743–748
45. B. Li, L. Li, B. Wang, C.Y. Li, Alternating patterns on single-walled carbon nanotubes. *Nature Nanotechnology*, 4 (2009) 358–362
46. B. Han, X. Yu, J. Ou, Multifunctional and smart nanotube reinforced cement-based materials. In *Nanotechnology in Civil Infrastructure. A Paradigm shift*. Gopalakrishnan K., Birgisson B., Taylor P., Attoh-Okine N. Editors – Springer (2011) 1-48
47. S.J. Chen, F.G. Collins, A.J.N. Macleod, Z. Pan, W.H. Duan, C.M. Wang, Review Paper. Carbon nanotube-cement composites: A retrospect, *The IES Journal Part A: Civil and Structural Engineering* (2011) 4(4) 254-265

48. J. Hilding, E.A. Grulke, Z.G. Zhang, F. Lockwood, Dispersion of carbon nanotubes in liquids. *Journal of Dispersion Science and Technology*, 24 (2003) 1–41
49. K.J. Loh, J. Gonzalez, Cementitious Composites Engineered with Embedded Carbon Nanotube Thin Films for Enhanced Sensing Performance. *Journal of Physics: conference Series* 628 (2015), 012042.
50. B. Han, S. Ding, X. Yu, Intrinsic self-sensing concrete and structures: A review. *Measurements* 59 (2015) 110-128
51. Y. Kuronuma, T. Takeda, Y. Shindo, F. Narita, Z. Wei, Electrical resistance-based strain sensing in carbon nanotube/polymer composites under tension: Analytical modeling and experiments. *Comp. Sci. Tec.* 72 (2012) 1678-1682
52. S. Gong, Z.H. Zhu, S.A. Meguid, Carbon nanotube agglomeration effect on piezoresistivity of polymer nanocomposites. *Polymer* 55 (2014) 5488-5499
53. C. Feng, L. Jiang, Micromechanics modeling of the electrical conductivity of carbon nanotube (CNT)-polymer nanocomposites. *Comp. A* 47 (2013) 143-149
54. B. Han, K. Zhang, X. Yu, E. Kwon, J. Ou, Electrical characteristics and pressure-sensitive response measurements of carboxyl MWNT/cement composites, *Cem. Concr. Comp.* 34 (2012) 794-800
55. R.K. Abu Al-Rub, A.I. Ashour, B.M. Tyson, On the aspect ratio effect of multi-walled carbon nanotube reinforcements on the mechanical properties of cementitious nanocomposites, *Constr. Build. Mater.* 35 (2012) 647-655.
56. T. Page McAndrew, P. Laurent, M. Havel, C. Roger, Arkema graphistrength® multi-walled carbon nanotubes, *Technical Proceedings of the 2008 NSTI Nanotechnology Conference and Trade Show, NSTI-Nanotech, Nanotechnology 2008* (2008), 1, pp. 47-50.
57. S. Wen, D.D.L. Chung, Double percolation in the electrical conduction in carbon fiber reinforced cement-based materials, *Carbon* 45 (2007) 263-267.